ARCHIVES
of
FOUNDRY ENGINEERING

ISSN (2299-2944)
Volume 2024
Issue 1/2024

66 – 79

9/1

10.24425/afe.2024.149253

Published quarterly as the organ of the Foundry Commission of the Polish Academy of Sciences

Characteristics of High-Strength Cast Steel Micro-Alloyed with Vanadium

B. Białobrzeska
Wrocław University of Technology, Poland
Corresponding author: E-mail address: beata.bialobrzeska@pwr.edu.pl

Received 22.11.2023; accepted in revised form 14.01.2024; available online 18.03.2024

Abstract

This article presents the results of research into the characteristics of cast steel alloyed with chromium and vanadium, subjected to heat treatment for increased strength parameters. In the first part, it discusses the state-of-the-art knowledge regarding technological developments in the field of cast-steel alloys and the influence of individual alloying additives on the microstructure and the properties of the steel alloy. Further sections present the results of microstructure observations performed with light microscopy, scanning electron microscopy, and transmission electron microscopy. This research focuses on the material in the state directly after casting and after heat treatment, which involved quenching and tempering at 200 °C. The microstructural analysis performed as part of this research has informed the discussion of the results obtained from tensile and impact strength tests. The article also includes the results of a fractography analysis performed as the final part of the tests and offers a general summary and conclusions.

Keywords: Vanadium, Low-alloyed cast steel, Heat treatment, Microstructure, Mechanical properties

1. Introduction

Recent developments in the field of material engineering and technologies which enable improved light alloy production and additive manufacturing have reversed the trend of marginalizing cast steel. The current potential of metallurgical and machining technologies allow the preparation of molds, and thus also casts, having complicated shapes. The possibility to develop original chemical compositions of cast steels opens way to designing materials having diverse properties that match the particular needs in various industry sectors. The elimination of the plastic forming stage from the production process also causes the price of cast steel to be competitive to the price of steel, making the former more advantageous in a broad range of applications. The use of cast steel eliminates or significantly reduces the need for welding and thus reduces the risk of unfavorable microstructural changes in the heat-affected zone, which could result in the warping or breaking of the object. The problem of welding high-strength structures has been discussed in [1]. Its authors describe the occurrence of breaks and warps due to the welding process and as a result recommend the use of high-strength cast steel in the manufacturing of arms for boom systems. The advantages of cast steel parts in structures which require the highest reliability and safety standards have been emphasized in [2]. It presents the application potential of cast steel as a structural material for steam turbine casings, ships, offshore structures or vehicle parts. Cast steel is not a novel material. Cast steels occurred in the industry already in the 1850s, when they were first produced in crucible furnaces. This is when the 2.5 tonne church bell was cast in the Bochum foundry. Over the next years, the economic growth, the increasing expectations of the customers, and the pursuit for profitability resulted in a significant qualitative and quantitative development of steel-casting processes. Modern casting methods were also introduced, such as converter (1856), open-hearth (1876), arc (1905) or induction furnaces. The end of the 19th century was also the time when annealing – one of the basic heat treatment procedures – was introduced. The mechanical properties

and application range of cast steels were further increased with the introduction of the subsequently developed casting processes: oxygen pressure casting and vacuum casting [3].

This group of materials includes a number of steel types, with the notable example of low-alloyed steels. Owing to their chemical composition and the applied heat treatment method, such cast steels can have strength properties comparable to the properties of steel. The remaining problem results from their ductility, which is lower than that of steel due to their microstructural properties specific to materials not subjected to plastic forming and their limitations, e.g. the presence of the primary microstructure, the segregation of the chemical composition or such casting defects as porosities and other discontinuities. Publication [4] notes that this ductility can be increased without compromising the strength parameters if low-alloyed cast steel is modified with mischmetal. Gajewski at al. [5] indicate another advantage of mischmetal additions. Rare earth metals were observed to reduce the content of sulfur in cast steel, and most importantly – to significantly modify the morphology of δ ferrite and non-metallic intrusions. In the case of austenitic steel, this phenomenon causes increased strength properties and a significant increase in the resistance to intergranular corrosion. As rare earth elements actively react with sulfur, nitrogen, carbon and other impurities present in steel, they form oxides, sulfides and oxide sulfides, modifying the amount, character and distribution of non-metallic intrusions. Numerous research works also focus on how modifications of cast steel influence the type, shape and size of intrusions [1].

Modifications and micro-alloying have been for years commonly used as methods for improving the properties of cast steels. Further developments of steel casting as well as improvements of the microstructure and mechanical properties of cast steels were enabled by the possibility to introduce modifications with particles having sizes on the order of nanometers and micrometers [6]. The typically used modifying particles include nitrides, carbides or borides having high melting temperatures (2000 °C – 3000 °C) and sizes between 4 and 100 nm. For example, tests performed by Lazarow et al. [6] indicate that the strength properties and ductility of cast steel increase after modification with nano and micro particles of TiCN. Numerous publications emphasize the advantages of adding small amounts of various elements, i.e. the so-called micro-additions. However, this influence is not explained by the modification of the crystallization process. Microadditions of Nb and V effect an increase in the mechanical properties of cast steel, particularly after heat treatment, and this increase is higher than expected from the modification degree of the chemical composition [7]. Although these elements are frequently added in small amounts, they significantly modify the microstructure and the properties of low-alloyed structural steel. L35GSM is an example of such cast steel, used in the construction of machines operated in lignite mines [8]. Vanadium added to steel shows strong affinity to carbon, nitrogen and oxygen and may form stable compounds with these elements. Vanadium is found typically as a carbide, and its main function is to refine the microstructure, thus reducing the proneness of steel to overheating and increasing its strength and ductility. Vanadium also increases the tempering stability of hardened steel and produces the secondary hardness effect. If it is not dissolved in austenite, it reduces the hardenability in general heat treatment conditions, and therefore it is often used together with manganese, chromium, molybdenum, tungsten and other elements in structural steels [9].

The possibility to obtain a low-alloyed cast steel having mechanical properties comparative to those of steel is thus very high, albeit the problems involved in the process are very complex. The technological process leading to high-quality cast steel requires high-purity charge materials as well as high technical culture and appropriate facilities in the foundry. It also requires knowledge about what effects in the microstructure are produced by the modifications or micro-alloying with particular elements. Such modifications and micro-alloying may for instance purify the alloy or improve its microstructure, thus improving its mechanical properties. Although cast steel has been discussed in numerous publications, some questions still remain about the complex effects produced by its modifying elements or alloying additives. Therefore, the aim of this study is to analyze the influence of vanadium and chromium added as complexing compounds to the FeCr 60 and FeV 70 cast steels on their microstructure and selected mechanical properties.

2. Materials and methods

The tests were performed for cast steel modified with chromium and vanadium. Its chemical composition is presented in Table 1. The ingot molds were prepared in bentonite mass, using wooden models of an agreed shape. The steel specimens of defined chemical compositions were cast in a Radyne 100 kW medium-frequency induction furnace with a capacity of 120 kg and inert lining. The mass of each batch was approximately 110 kg. The defined chemical composition was maintained by blowing argon under a hood-type structure installed above the crucible. The melt batch comprised ARMCO iron, low-carbon scrap steel, the following additives: FeMn 80, FeCr 60, Mn, FeV 70, Al, Ti, and carburizer. After the batch had been molten and the temperature readings had been taken, a specimen for assays was collected. If needed, the components that could burn-out were added just before casting. The molten metal was cast into a preheated ladle, the temperature was measured and a specimen was collected for assays of the final product. The casting temperature was 1540 °C. The ingots were cooled and cleaned from the mass, and the risers were removed. The ultrasound tests were performed with the use of the CUD 9900 No. 04002 defectoscope (provided with the 2x4L02 No. U07134 head, measurement range 0;150 mm, amplification 48 dB). The tests did not reveal any disqualifying defects.

The chemical composition presented in Table 1 was tested using the ARL NA optical spark emission spectrometer. The content of trace elements was measured using the atomic absorption spectrometry method, in the Solaar M6 Thermo spectrometer.

Table 1.
Chemical composition of the analyzed cast steel, in %weight (nitrogen expressed in ppm)

C	Si	Mn	P	S	Cr	Ni
0.37	0.45	1.40	0.017	0.009	0.970	0.075
Mo	Cu	V	Ti	Al	B	N
0.020	0.060	0.275	0.008	0.022	0.0003	62

The ingots served as sources of cuboid specimens which were subjected to a homogenizing treatment (austenitizing temperature was 1200 °C, austenitizing time 1 hour, cooling together with the furnace) and then normalized (austenitizing temperature 900 °C, austenitizing time 1 hour, cooling in the open air) in order to reduce the grain size. The normalized specimens were mechanically processed until they met the required dimensions. They were subsequently austenitized for 30 minutes. The austenitizing temperature was selected on the basis of dilatometric tests performed with the use of the Linseis L78 R.I.T.A. dilatometer in order to determine the A_{c3} temperature. The austenitizing temperature was 870 °C and was higher by 50 °C than the A_{c3} temperature. Upon the completion of the austenitizing process, the specimens were quenched in the Durixol W72 quenching oil having a kinematic viscosity of 21 mm^2/s, and a temperature of 50±5 °C, and then tempered for 2 hours at 200 °C. The high-temperature operations were performed in the Czylok FCF 12SHM/R gas-tight chamber furnace, in a 99.95 % argon protective atmosphere.

The microstructure of the analyzed alloys was inspected under the Nikon Eclipse MA200 light microscope and under the scanning electron microscopes Phenom XL (with the backscatter detector and a 15 kV acceleration voltage) and Versa 3D (with the Everhart-Thornley detector and a 20 kV acceleration voltage). The inspection was performed after the specimens were etched with a 3% solution of HNO3 in ethyl alcohol, as per the ASTM E407 standard. Additional observations were performed with the use of the transmission electron microscope Tecnai G2 20 TWIN provided with a high angle annular dark field detector (HAADF) and coupled with an EDAX energy dispersive x-ray spectrometer. The specimens were prepared by forming thin foils with Ga+ ions in the Quanta 3D 200i focused ion beam (FIB) device manufactured by FEI and equipped with an ion gun on the basis of a scanning microscope.

The static tensile tests were performed in ambient temperature and based on the current EN ISO 6892-1:2019 standard. The test specimens were fivefold cylindrical specimens with a circular cross-section having a diameter d = 10 mm and a measurement base length L_0 = 50 mm typical for this type of strength tests. The specimens distributed symmetrically on the cross-section of the ingot were collected along the axial direction of the specimens, which was consistent with the longitudinal axis of the ingot. One ingot thus served as a source of 18 specimens for tensile tests. The tests were performed on the MTS 810 machine provided with an extensometer having a set measurement base length L_0 = 50 mm. The tests involved series of a minimum of 3 specimens for all of the analyzed conditions of the material. The tensile tests were performed at a constant extension speed controlled on the basis of the stress increment rate (method B as per the above standard), until failure. The test results provided basic material strength properties: offset yield or yield point ($Rp_{0.2}$ or R_e) and tensile strength (R_m) as well as plastic properties: percent elongation (A) and percent reduction in area (Z) at fracture.

The Charpy impact strength tests were performed with the Zwick Roell RPK300 hammer, with an initial energy of 300 J, as per PN-EN ISO 148-1:2017-02. The specimens used in the tests were standard cuboids with "V" notches. The specimens distributed symmetrically on the cross-section of the ingot were collected along the axial direction of the specimens, which was consistent with the longitudinal axis of the ingot. The tests were performed at -40 °C, -20 °C, 0 °C, +20 °C, after the specimens had been conditioned for 15 minutes in a mixture of liquid nitrogen and methanol. The temperature was measured with the Center 309 digital thermometer. The tests involved series of a minimum of 3 specimens for all of the analyzed conditions of the material and temperatures. The fractographic inspection was performed on unetched specimens, with the Nikon AZ100 multifunction stereoscopic microscope and with the Phenom XL scanning electron microscope (with a secondary electron detector and a 15 kV acceleration voltage).

The hardness tests were performed following the Brinell method, with the Zwick/Roel ZHU 187.5 universal tester, in accordance with PN-EN ISO 6506-1:2014-12. They employed a sintered carbide ball 2.5 mm in diameter, with a load of 187.5 kgf (1838,7469 N) applied for 15 s.

The test results were averaged, and the confidence limits and standard deviation were identified following the Student's t-distribution.

3. Results and discussion

The microstructure in the condition directly after casting comprised ferrite and high-dispersion perlite (Figs. 1a and 1b). The content of perlite was significant and higher than would result from the carbon percentage. A limited amount of ferrite was distributed in the form of a thin network and inside the perlite grains (Fig. 1a). After the homogenizing treatment, the content of ferrite in the microstructure significantly increased. It was arranged mainly in large groups, forming colony-type structures, with occasional, local networks around perlite grains (Fig. 2a). The microstructure was similar to the equilibrium microstructure and the content of its individual components corresponded to the content of carbon in the cast steel. After the normalization process, numerous microstructural changes were observed in the analyzed cast steel. The microstructure was varied, comprising mainly laths of ferrite supersaturated with carbon, i.e. of lower bainite (the dark laths) or quenched martensite (light laths), upper bainite, grain boundary ferrite (allotriomorphic ferrite) and high-dispersion perlite (troostite or sorbite) (Fig. 2b). Morphologically, martensite and bainite form packets with very low variability of crystallographic orientation, affecting only blocks within the grain boundaries of the former austenite. Such diffusionless structures occurred due to the hardening processes already during the cooling of the cast steel in air. Small areas, probably of retained austenite, could be observed between the ferrite laths. After quenching in oil, the microstructure comprised only diffusionless structures, i.e. fine laths of quenched martensite with a typical,

clearly hierarchical microstructure composed of blocks and packets within the clearly marked grain boundaries of the former austenite (Fig. 3a). Moreover, primary vanadium carbides (VC) were also observed (Fig. 3b) and identified with transmission electron microscopy techniques (Figs. 4a, 4b, 5). These techniques also allowed observations of small retained austenite areas, deformation twins and defects manifested as dislocation lines occurring between the martensite laths (Fig. 4a). Twin martensite is formed during the process of cooling below temperature M_S in unstressed conditions, and the twin domains are observed on the level of grain size, having crystallographic characteristics different only for the local orientation. The tempering process initiated diffusion processes in the analyzed cast steel, and these entailed the formation of high-dispersion secondary carbides typical of this tempering temperature (Fig. 6a and 6b).

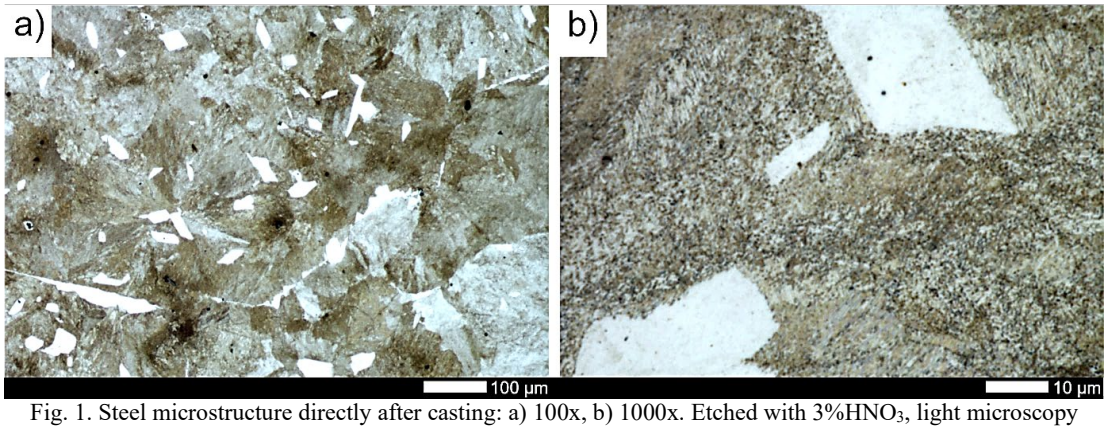

Fig. 1. Steel microstructure directly after casting: a) 100x, b) 1000x. Etched with 3%HNO_3, light microscopy

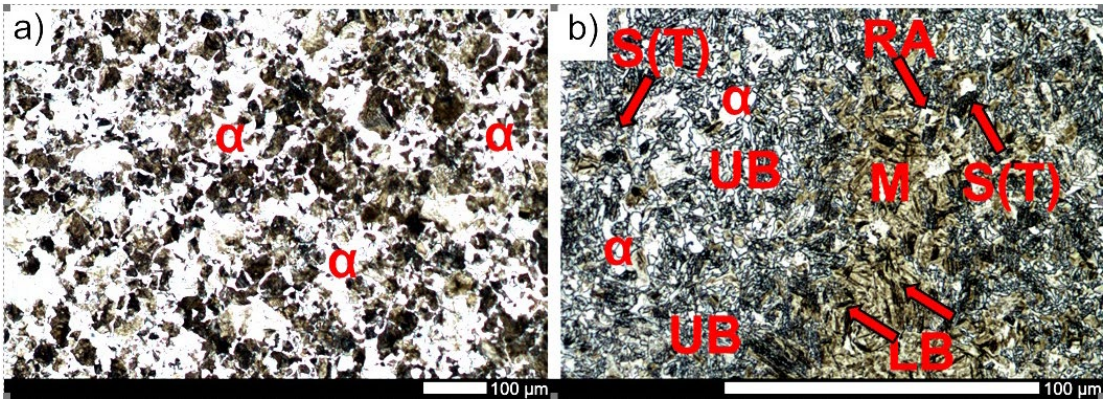

Fig. 2. Steel microstructure after annealing: a) homogenizing, b) normalizing. Etched with 3%HNO_3, light microscopy. α – ferrite, LB – low bainite, UB – upper bainite, M – martensite, S(T) – sorbite(troostite), RA – retained austenite

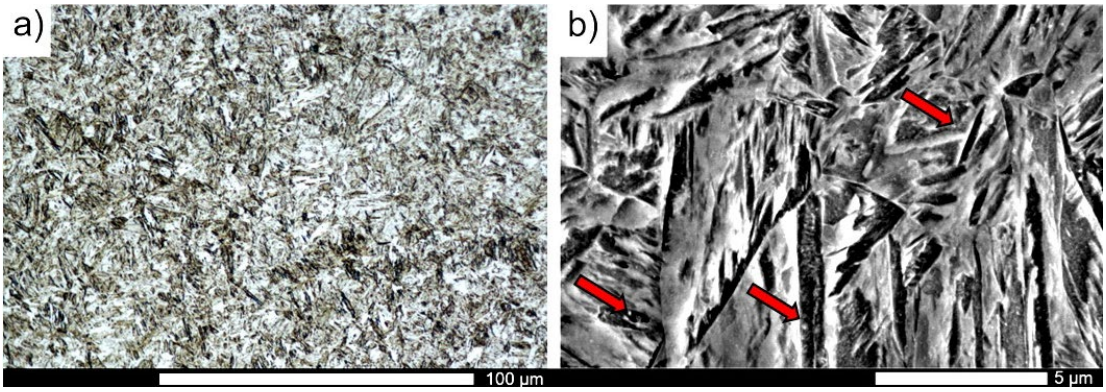

Fig. 3. Steel microstructure after quenching: a) light microscopy, b) SEM. Etched with 3%HNO_3. Arrows indicate example vanadium carbides

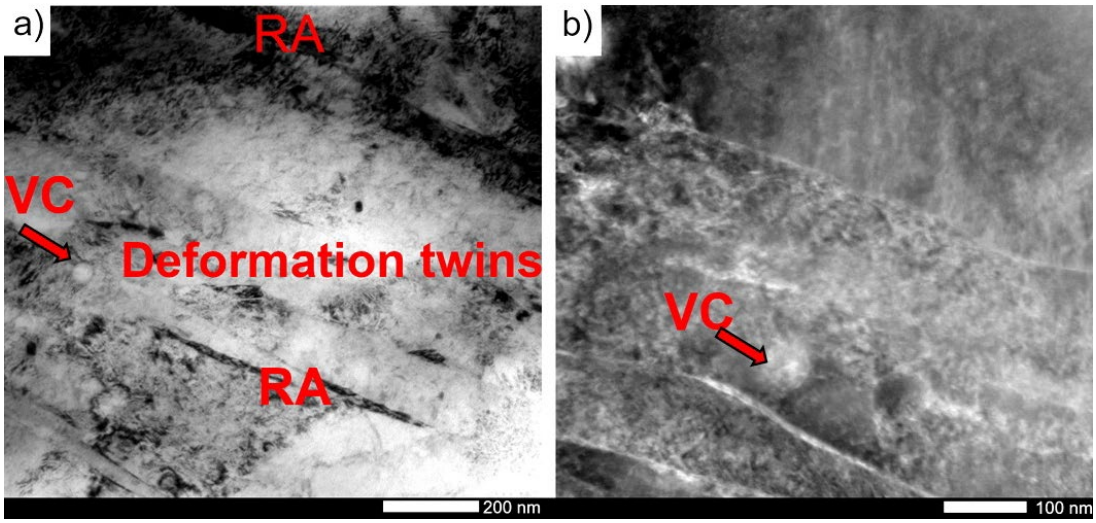

Fig. 4. Martensitic structure of cast steel a) dark field, b) annular dark field detector. The arrow indicates a carbide subjected to EDAX analysis. Etched, TEM. VC – vanadium carbides, RA – retained austenite

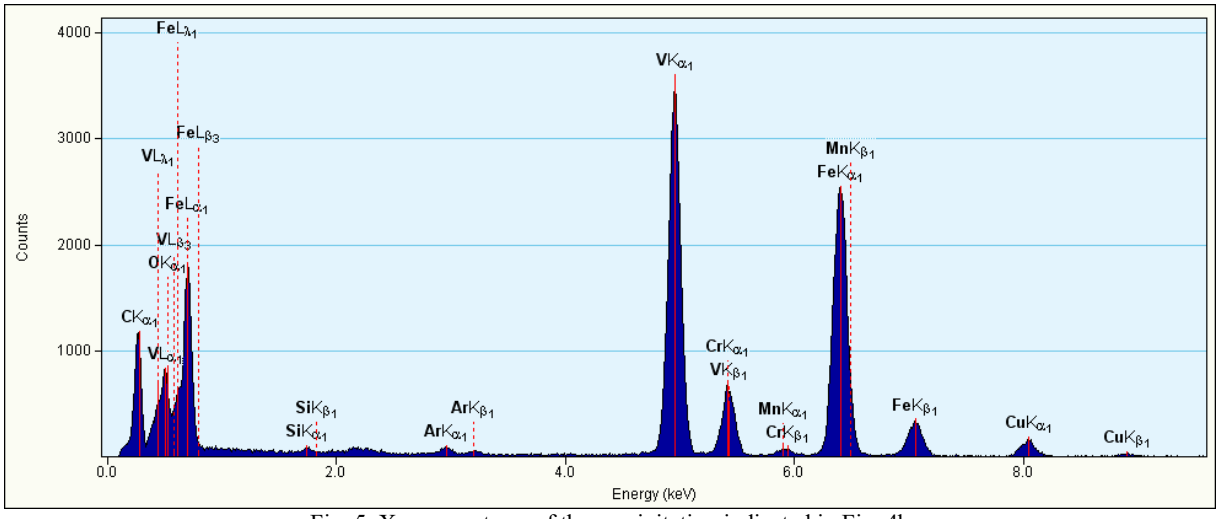

Fig. 5. X-ray spectrum of the precipitation indicated in Fig. 4b

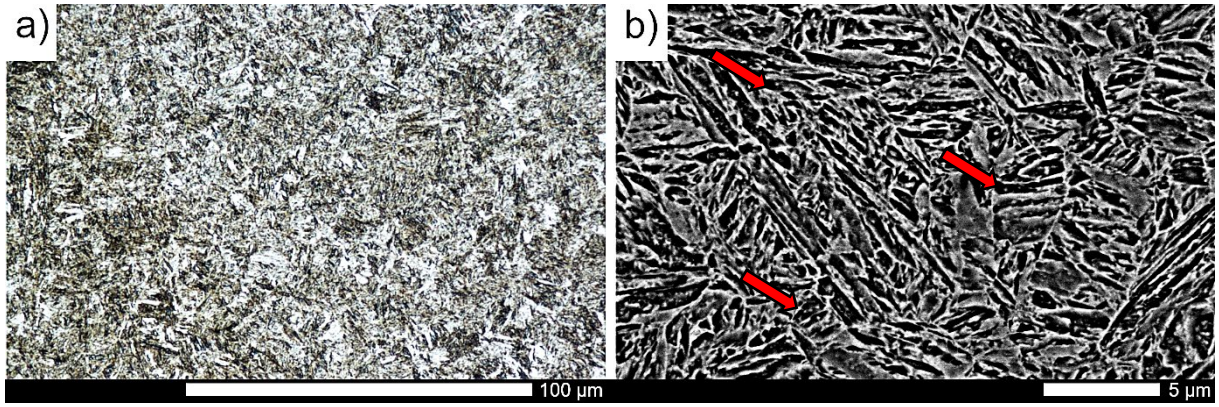

Fig. 6. Steel microstructure after quenching and after tempering at 200 °C: a) light microscopy, b) SEM. Etched with 3%HNO_3. Arrows indicate secondary carbides

Fig. 7 aggregates the mechanical properties measured in the static tensile tests and hardness tests of the steel in the as-cast condition and after an extensive heat treatment comprising homogenizing treatment, normalization, quenching and low tempering. For comparison purposes, Fig. 8 shows characteristic curves representing the results of static tensile tests performed for the two steel conditions. Interestingly, in the as-cast condition, the material demonstrated low strength properties and insufficient ductility. In this condition, its hardness was 308 HBW and its yield point was 554 MPa. Such parameters as percent elongation and reduction in area after fracture were low: 3.0 and 0.5 %, respectively. They clearly indicate that the obtained material properties are typical of the brittle state. After the extensive heat treatment, the values of both strength and plastic indicators increased. In this condition, steel hardness was 557 HBW, and yield point was 1483 MPa, with percent elongation and reduction in area after fracture at 6 and 7%, respectively. Such high strength parameters suggest that it was appropriate to perform the normalization process in order to reduce the grain size and obtain a fine-lath microstructure in the quenching procedure. However, low values of percent elongation and reduction in area allow the material to be defined as brittle under static loads. Of fundamental importance here is the reduction, which is a more stringent criterion in determining the brittleness of a material [10]. It should be noted that the value of this parameter has increased significantly compared to the as-cast state, which requires further analysis. Therefore, additional impact load tests were performed, and supplemented with tests at low temperatures with detailed fractographic analysis.

The results of these tests are shown in Fig. 9. In the as-cast condition, the impact strength was below satisfactory across the entire test temperature range. In room temperature, it was minimally above 3.5 J/cm^2, and in lower temperatures it was within 2.4-2.9 J/cm^2. Such an impact strength clearly indicates that the material is prone to brittle cracking. Although after the extensive heat treatment the values of the impact strength improved, they still remained below satisfactory levels. The material brittleness threshold is identified following various criteria. One such frequently applied criterion is an arbitrarily assumed certain value of impact energy or impact strength. For structural steels, this impact strength value is assumed as equal or close to 35 J/cm^2 [11]. From the proposed quantitative evaluation perspective, the analyzed cast steel after heat treatment was also prone to brittle cracking. The impact strength in room temperature was approximately 14 J/cm^2 and did not practically decrease even at 0 °C. Moreover, although the results demonstrate the highest variability, with the coefficients of variation at 40% they remained within the average range. A gradual decrease of the impact strength, to approx. 9 and 7 J/cm^2 was observed as a result of lowering the temperature of the impact resistance test, to -20 °C and -40 °C, respectively. Importantly, documentation regarding structural materials advises the upper limit of critical brittleness range with sufficient ductility to be located in temperatures higher than the operating temperature, frequently in room temperature.

The macroscopic analysis in the as-cast condition (Fig. 10) has confirmed this quantitative evaluation. The obtained typical cleavage fractures had coarse surfaces resulting from the size of the crystallites. On the other hand, observations of specimens after heat treatment confirmed the presence of relatively large plastic regions, observed in the final fracture zones and under the mechanical notch, as well as relatively wide, plastically deformed side regions (Fig. 11). The above observations apply primarily to the fracture obtained in the room temperature test, in which the share of plastic zones in the fracture was at approx. 25%. The macroscopic observations, also in the condition after heat treatment, have thus confirmed the obtained results, as the brittleness criterion, which for structural steel is at the impact strength level of 35 J/cm^2, corresponds to a semi-brittle and semi-ductile fracture.

The fractographic microanalysis was performed in three typical locations, i.e. under the mechanical notch, in the central part of the specimen, and on the side opposite to the mechanical notch. The results are presented in Figs. 12-14. For graphic reasons, the microphotographs have been rotated by -90°, so that the mechanical notch is on the left side of the photograph. In the case of steel not subjected to heat treatment, the microstructures of the fracture surfaces in each of the regions were similar and had distinctive characteristics of a brittle transcrystalline fracture – a set of steps of various sizes (although fractures along the grain boundaries were also observed) (Fig. 12). Such a cleavage occurs when a fracture propagates along certain crystallographic planes of the grain. Cleavage facets correspond to the size of the crystallites and contain characteristic steps formed in a river pattern. The zone opposite to the mechanical notch is the only area in which the steps become finer and less sharp, with an increasing number of secondary fractures penetrating inwards and away from the surface (Fig. 12c). Importantly, cleavage fractures in pearlitic steels are characteristic in that their elementary surface typically depends on the size of the former austenite grain and may traverse several pearlite colonies [12]. The steps are due to grain boundaries, which prevent the cleavages from propagating further and from shifting from one cleavage plane to another. Namely, the step occurs if the front of the fracture encounters a screw dislocation. In such case, the propagation direction of the main fracture changes and its propagation is locally delayed, eventually leading to the combination of the adjacent steps into a system of rivers and tributaries [13]. In some systems, the steps are also arranged radially, in the so-called fan-type pattern (Fig. 12b). As a result, the fracture propagates from one point in all directions, with characteristic tongue steps. Interestingly, some regions resemble tire trucks (Fig. 12a), although the author of this article hesitates to use such terminology, as the indentation marks are typical of a fatigue fracture [12].

The material after heat treatment had a different fracture line (Figs. 13 and 14). After the room-temperature test, the region under the mechanical notch was a ductile fracture of a characteristic dimple structure (Figs. 13a and 14). Such a structure is formed from micropores or microfractures which propagate until they become connected. The very fracture propagation process depends on the size of the martensite laths and therefore the elementary separation surfaces were smaller than in the case of cast steel having pearlitic structure [12]. Non-metallic intrusions could be observed in some of the dimple bottoms. The majority of the dimples were fine and shallow, but individual large and deep dimples also occurred. Importantly, the larger and deeper the dimples, the more ductile the material. The dimples were also uniformly distributed, indicating a similar fracture

propagation speed in individual parts of the fracture. The dimple-shaped structure was also evident in the central zone. Moreover, the steps on the fracture surfaces were also very small, and in some cases they were completely smooth, forming extremely brittle fractures, as if impressed in the plastic base, as well as small regions of quasi-cleavage fracture (Fig. 14b). Such a fracture is formed when small, local brittle fractures subsequently combine into one fracture surface due to plastic deformations. Although the river pattern causes the quasi-cleavage facets to resemble cleavage facets, the identification of crystallographic planes is in this case almost impossible. The zone opposite to the mechanical notch was also observed to have typical characteristics of a mixed-type fracture containing a ductile fracture with varied number of dimples and a quasi-cleavage fracture (Fig. 14c). Importantly, the topography of the fracture in each specimen was relatively well-developed, with a characteristic relief of rises, whose walls comprised strips of very fine dimples (Fig. 13). Such a topography implies that the fracture did not propagate in one crystallographic plane but rather shifted from one plane to another by shear or secondary cracks of the dividing walls. In temperatures below 0 °C, each zone of the specimen showed an evident structure typical of a quasi-cleavage fracture, with the characteristic tear ridges (Figs. 14c, 14d, 14f). The share of ductile fragments was limited and mainly in regions with very fine dimples. The topography of the fracture was still well-developed, with a characteristic pattern of rises (Figs. 13d, 13e, 13f). It is noteworthy that the results of fractographic examination correspond with the results available in the literature for steel of similar class, particularly with respect to the temperature ranges above 0 °C (ductile fracture with elements of quasi-cleavage fracture) and also below 0 °C, in which the material retains its plastic properties. Described micromechanisms of deformation process are summarized in table 2.

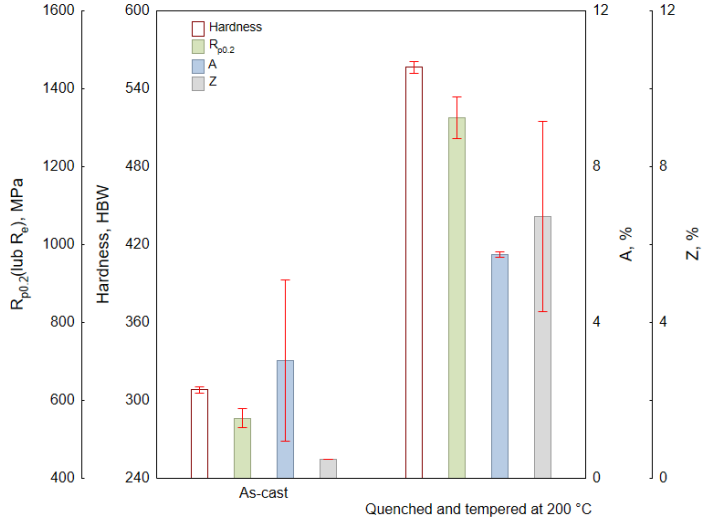

Fig. 7. Selected mechanical properties of cast steel for as-cast steel and for steel quenched and tempered at 200 °C

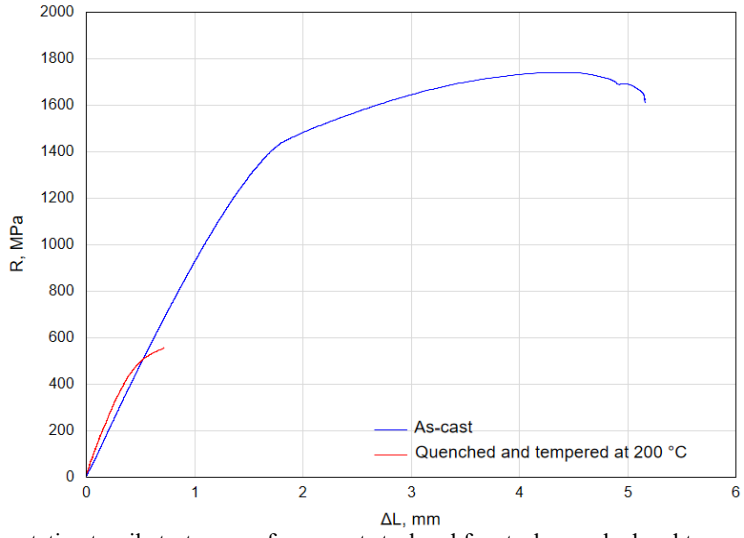

Fig. 8. Representative tensile test curves for as-cast steel and for steel quenched and tempered at 200 °C

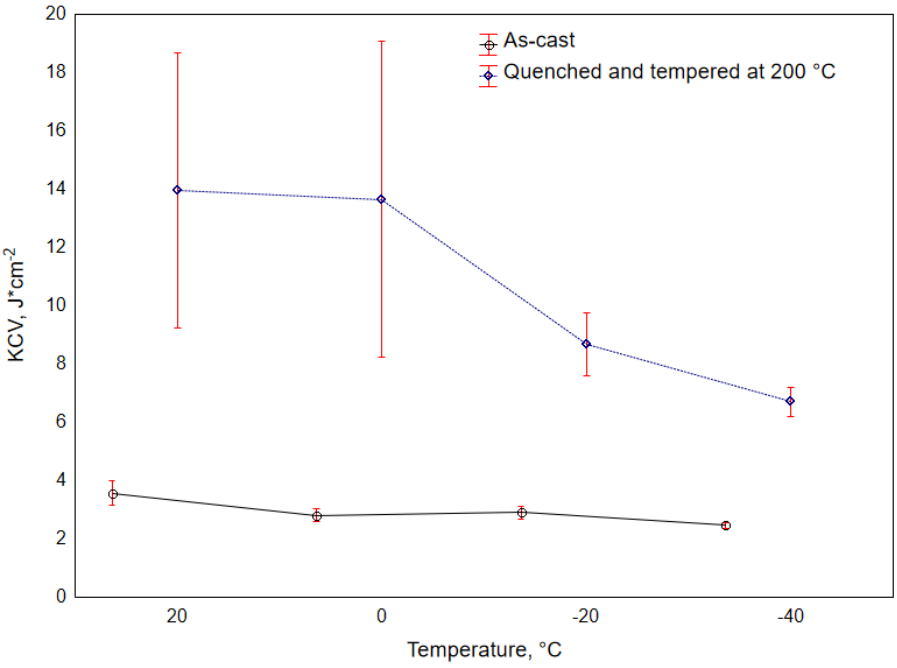

Fig. 9. Impact strength versus temperature for as-cast steel the for steel quenched and tempered at 200 °C

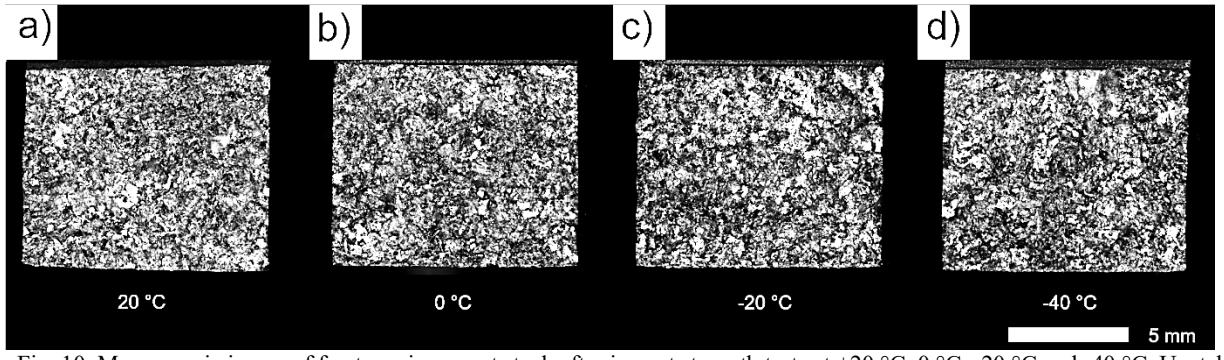

Fig. 10. Macroscopic image of fractures in as-cast steel, after impact strength tests at +20 °C, 0 °C, -20 °C and -40 °C. Unetched condition, stereoscopic microscopy

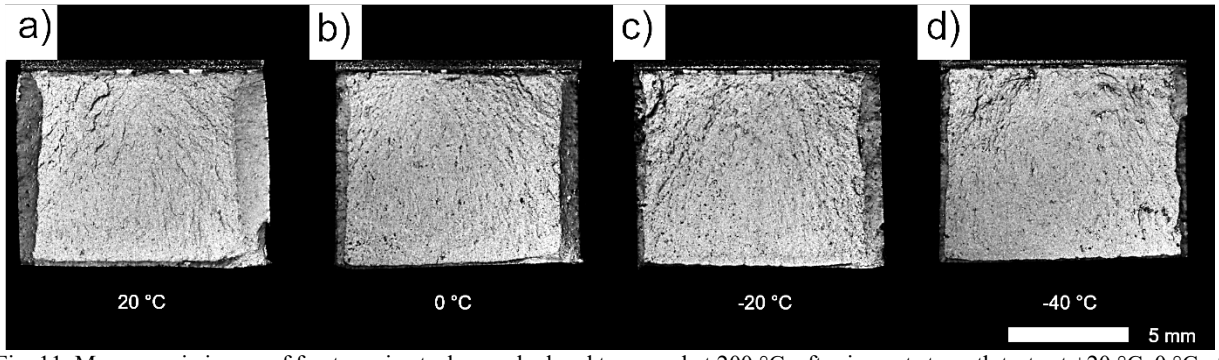

Fig. 11. Macroscopic image of fractures in steel quenched and tempered at 200 °C, after impact strength tests at +20 °C, 0 °C, -20 °C and -40 °C. Unetched condition, stereoscopic microscopy

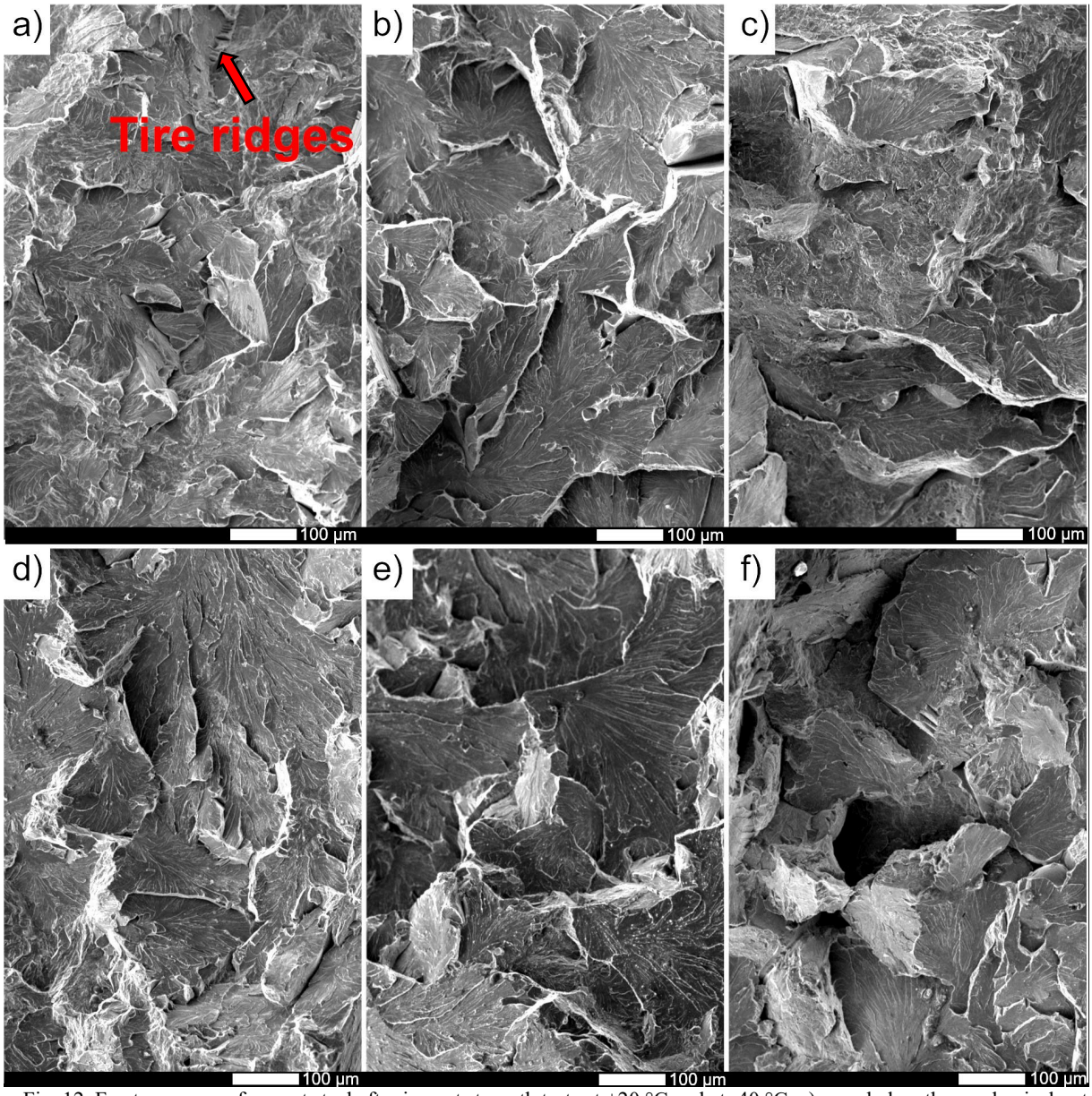

Fig. 12. Fracture zones of as-cast steel after impact strength tests at +20 °C and at -40 °C: a) zone below the mechanical notch, +20 °C, b) central zone, +20 °C, c) zone opposite to the mechanical notch, +20 °C, d) zone under the mechanical notch -40 °C, e) central zone, -40 °C, f) zone opposite to the mechanical notch, -40 °C. Unetched condition, SEM

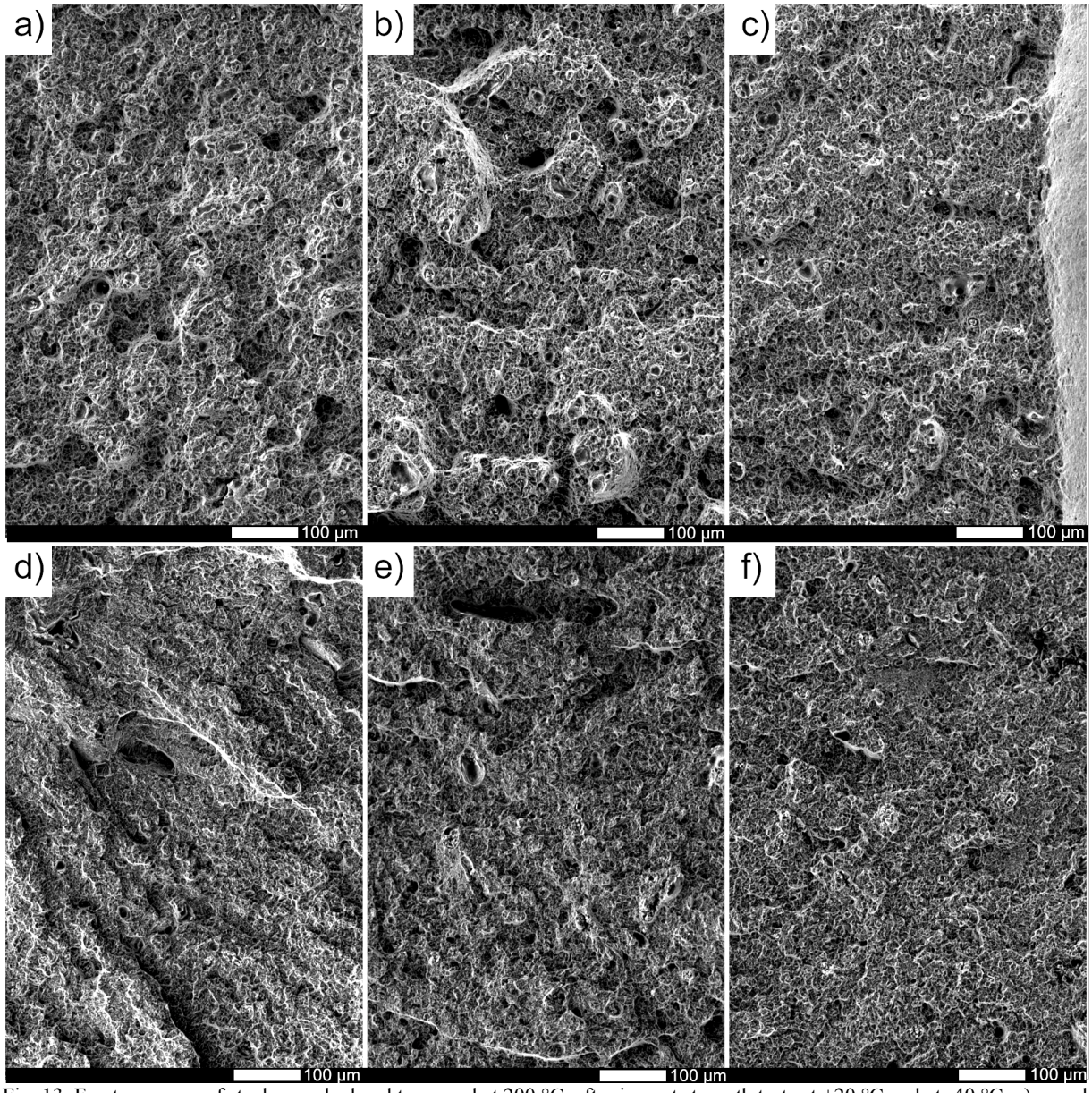

Fig. 13. Fracture zones of steel quenched and tempered at 200 °C, after impact strength tests at +20 °C and at -40 °C: a) zone below the mechanical notch, +20 °C, b) central zone, +20 °C, c) zone opposite to the mechanical notch, +20 °C, d) zone under the mechanical notch -40 °C, e) central zone, -40 °C, f) zone opposite to the mechanical notch, -40 °C. Unetched condition, SEM

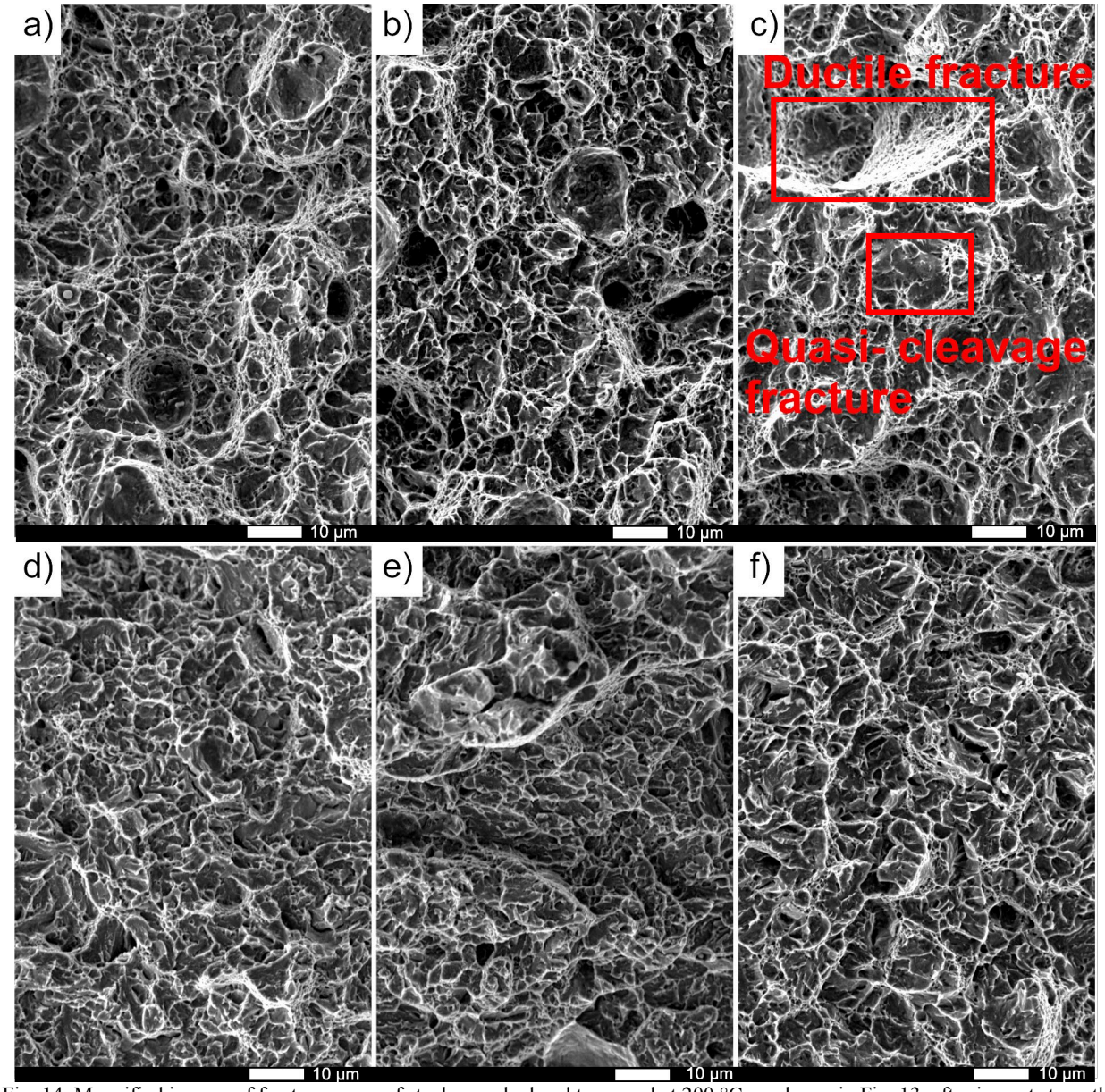

Fig. 14. Magnified images of fracture zones of steel quenched and tempered at 200 °C, as shown in Fig. 13, after impact strength tests at +20 °C and at -40 °C: a) zone below the mechanical notch, +20 °C, b) central zone, +20 °C, c) zone opposite to the mechanical notch, +20 °C, d) zone under the mechanical notch -40 °C, e) central zone, -40 °C, f) zone opposite to the mechanical notch, -40 °C. Unetched condition, SEM

Table 2.
Micromechanisms of deformation process

Zone of the specimen	Micromechanisms of deformation process
As-cast state, temperature +20 °C and -40 °C	
Below the mechanical notch	Brittle transcrystalline fracture, characteristic steps formed in a river or fan-type pattern (some intercrystalline cracks), tear ridges, tongue steps
Center	Brittle transcrystalline fracture characteristic steps formed in a river or fan-type pattern (some intercrystalline cracks)
Opposite to the mechanical notch	Brittle transcrystalline fracture characteristic steps formed in a river or fan-type pattern (some intercrystalline cracks), patters are finer and less sharp, numerous secondary fractures
Heat-treated state, temperature +20 °C	
Below the mechanical notch	Ductile fracture of a characteristic dimple structure with non-metallic inclusions, majority of the dimples were fine and shallow, but individual large and deep, well-developed topography
Center	Ductile fracture with small steps, some smooth forming completely brittle fracture, small regions of quasi-cleavage fracture, well-developed topography
Opposite to the mechanical notch	Typical features of a mixed fracture, namely, ductile with varying size of dimples and quasi-cleavage, well-developed topography
Heat-treated state, temperature -40 °C	
Below the mechanical notch	Quasi-cleavage fracture with typical tear ridges, small areas of ductile fracture consisted of with very fine dimples, well-developed topography with a characteristic rises spreading radially from the initiation point of the fracture
Center	Quasi-cleavage fracture with typical tear ridges, small areas of ductile fracture consisted of with very fine dimples, well-developed topography
Opposite to the mechanical notch	Quasi-cleavage fracture with typical tear ridges, small areas of ductile fracture consisted of with very fine dimples, well-developed topography

The analyzed as-cast steel has low mechanical properties, in particular the resistance to dynamic loads, and thus has a limited application potential. However, vanadium has an evidently positive effect on the strength parameters of cast steel, which fact is consistent with the observations of Kaladyk et al. [14]. The full potential of the added alloying elements was obtained only after extensive heat treatment, which caused significant modifications, particularly of the strength properties [15] [16]. In practice, the addition of 0.1% of vanadium to structural steel may increase its strength by 10-20%, reduce its structural weight by 15-25%, and reduce its cost by 8-10%, and in the case of high-strength steel the weight of the metal structure can be reduced by as much as 40-50% [9]. Most types of steels comprising vanadium are structural steels with a medium carbon content (0.2-0.5%), a tensile strength of 490-1200 MPa and good ductility. In order to comprehensively improve the properties of such steels (tensile strength, ductility and impact strength), the quenching step is typically followed by tempering in high temperature. On the other hand, typical steels with medium carbon content, intended for heat treatment comprising tempering in low temperatures, contain not only vanadium but also such alloying additives as Cr, Ni and Mo. This group also includes steels defined as high-strength or ultra-high-strength medium-carbon steels, of such types as 30M, 4340V, D6AC, 4330V. For example, steel D6AC reaches the hardness of 53 HRC, the tensile strength of 1931 MPa, and the yield point above 1700 MPa with a 7% relative elongation. Although during the analysis of the strength properties the focus has been only on the yield point, the tensile strength for the analyzed cast steel was observed at 1800 MPa. The properties of the cast steel can be thus described as satisfactory in comparison to the properties even of such high-strength steels subjected to specialist plastic processing which most likely involves thermomechanical rolling carefully controlled by the manufacturer. Cast steel may be therefore applied for example in working elements subjected to abrasive wear processes. Note should be made here that low-alloyed cast steel types with increased wear resistance are frequently used for elements of heavy-duty machines such as continuous mining machines, loaders, mills etc. [17]. Importantly, the mechanical properties of the analyzed cast steel should be considered in the context of the properties of other casting alloys. The entire group discussed above is well represented by cast steel L20HGSNM as per PN-H-83160:1988 which has the highest mechanical properties (Rm > 1300 MPa and Re> 1100 MPa) of all cast steel types listed in Polish Standards [17]. The strength properties of cast steel L20HGSNM are in many cases insufficient. Therefore, attempts are justified to modify the material composition or its technological process so as to increase these properties at, also importantly, relatively low cost [18]. Such attempts have been made for example by Szajnar et al. [17], who obtained a cast steel having the strength of 1450 MPa. In the view of such successes, further research on the analyzed group of cast steels seems justified. Such research will concentrate on the comparative

analysis of the influence of chromium and vanadium on the temperability of cast steels, which will be supplemented with the evaluation of the influence of these elements on the mechanical properties of steel, with particular emphasis on impact strength in other states of thermal treatment. Attempts will also be made to improve ductility without sacrificing the high strength parameters of cast steel.

4. Conclusions

The analysis of the above test results has allowed the formulation of the following conclusions:

1) Cast steel modified with ferrochromium and ferrovanadium in as-cast condition has a pearlitic-ferritic microstructure in which ferrite is distributed in the form of a thin network and inside the pearlite grains. On the other hand, the content of perlite was higher than would result from the carbon percentage content. After the homogenizing treatment, the microstructure was similar to equilibrium microstructure and the content of its individual components corresponded to the content of carbon in the cast steel. The microstructure of normalized cast steel comprised mainly laths of ferrite supersaturated with carbon, i.e. of lower bainite (the dark laths) or hardened martensite (light laths), upper bainite, grain boundary ferrite (allotriomorphic ferrite) and high-dispersion perlite (troostite or sorbite). The quenching in oil resulted in the formation of fine laths of quenched martensite with a typical, clearly hierarchical structure together with primary vanadium carbides (VC). The tempering process initiated the precipitation of low-dispersion secondary carbides typical of this tempering temperature.
2) In the as-cast condition, the steel had low mechanical properties, in particular low impact strength within the entire temperature range of the test. Heat treatment effected a significant increase in the values of strength parameters, while the indicators of the material ductility remained at an insufficient level.
3) The fractographic analysis demonstrated significant differences in the morphology of the fractures for the two investigated states of cast steel alloyed with chromium and vanadium. The fracture after heat treatment had more advantageous characteristics, showing a mixed-type structure typical of a ductile and quasi-cleavage fracture.
4) Homogenizing heat treatment (austenitizing temperature: 1200 °C, austenitizing time: 1 hour, cooling with the furnace) followed by normalization (austenitizing temperature: 900 °C, austenitizing time: 1 hour, cooling in air), quenching (austenitizing temperature: 870 °C, austenitizing time: 30 minutes, cooling in oil) and tempering (temperature: 200 °C, duration: 2 hours, cooling in air) produces cast steel having high strength parameters, i.e. the hardness of 557 HBW and the yield point of 1483 MPa with percent elongation and reduction in area after fracture at 6 and 7%, respectively.

4. References

[1] Bartocha, D., Kilarski, J., Suchoń, J., Baron, C., Szajnar, J. & Janerka, K. (2011). Low-alloy constructional cast steel. *Archives of Foundry Engineering*. 11(spec.3), 265-271. ISSN (1897-3310). (in Polish).

[2] Skołek, E., Szwejkowska, K., Chmielarz, K., Świątnicki, W. A., Myszka, D. & Wieczorek, A.N. (2022). The microstructure of cast steel subjected to austempering and B-Q&P heat treatment. *Metallurgical and Materials Transactions A: Physical Metallurgy and Materials Science*. 53(7), 2544-2560. https://doi.org/10.1007/s11661-022-06685-3.

[3] Kniaginin, G. (1977). Cast steel: Metallurgy and foundry. Katowice: Wydawnictwo "Śląsk". (in Polish).

[4] Sobula, S., Tęcza, G., Krasa, O. & Wajda, W. (2013). Grain refinement of low alloy Cr-Mn-Si-Ni-Mo cast steel with boron, titanium and rare elements additions. *Archives of Foundry Engineering*. 13(3) 153-156. ISSN (1897-3310). (in Polish).

[5] Gajewski, M. & Kasińska, J. (2012). Effects of Cr - Ni 18/9 austenitic cast steel modification by mischmetal. *Archives of Foundry Engineering*. 12(spec.4), 47-52. DOI: 10.2478/v10266-012-0105-y.

[6] Lazarova, R., Petrov, R.H., Gaydarova, V., Davidkov, A., Alexeev, A., Manchev, M. & Manolov, V. (2011). Microstructure and mechanical properties of P265GH cast steel after modification with TiCN particles. *Materials & Design*. 32(5), 2734-2741. DOI: 10.1016/J.MATDES.2011.01.024.

[7] Yang, S.Z. (2010). *Vanadium Metallurgy.* Beijing: Metallurgical Industry Press.

[8] Dobrzański, L.A. (2002). *Fundamentals of materials science and metal science*. Warszawa: Wydawnictwo Naukowo-Techniczne. (in Polish).

[9] Baoxiang, Y., Jinyong, H., Guifang, Z. & Jike, G. (2021). Applications of vanadium in the steel industry. *Vanadium.* 267-332. DOI: 10.1016/B978-0-12-818898-9.00011-5.

[10] Panin, S.V., Maruschak, P.O., Vlasov, I.V., Syromyatnikova, A.S., Bolshakov, A.M., Berto, F., Prentkovskis, O. & Ovechkin, B.B. (2017). Effect of operating degradation in arctic conditions on physical and mechanical properties of 09Mn2Si pipeline steel. *Procedia Engineering*. 178, 597-603. https://doi.org/10.1016/j.proeng.2017.01.117.

[11] Wyrzykowski, J.W., Pleszakow, E. & Sieniawski, J. (1999). *Deformation and cracking of metals*. Warszawa: Wydawnictwo Naukowo-Techniczne. (in Polish).

[12] Kocańda, S. (1972). *Fatigue destruction of metals*. Warszawa: Wydawnictwo: Naukowo-Techniczne. (in Polish).

[13] Maciejny, A. (1973). *Brittleness of metals*. Katowice: Wydawnictwo "Śląsk". (in Polish).

[14] Kalandyk, B. & Zapała, R. (2008). Effect of heat treatment parameters on the properties of low-alloy cast steel with microadditions of vanadium. *Archives of Foundry Engineering*. 8(3), 137-140. ISSN(1897-3310).

[15] Kalandyk, B., Sierant, Z. & Sobula, S. (2009). Optimisation of microstructure, yield and impact strength of carbon cast

steel by vanadium additions. *Przegląd Odlewnictwa*. 59(3), 108-113. (in Polish).
[16] Kalandyk, B. & Głownia, J. (2003). Influence of V and Mo and heat treatment of constructional Mn–Ni cast steels acquirement of yield strength above 850MPa. *Archiwum Odlewnictwa*. 3(8), 69-74. (in Polish). ISSN 1642-5308.
[17] Szajnar, J., Studnicki, A., Głownia, J., Kondracki, M., Suchoń, J. & Wróbel, T. (2013). Technological aspects of low-alloyed cast steel massive casting manufacturing. *Archives of Foundry Engineering*. 13(4), 97-102. ISSN (1897-3310).
[18] Sobula, S., Rąpała, M., Tęcza, G., & Głownia, J. (2009). Cast steels of a yield strength above 1300 MPa comparable to forgings. *Przegląd Odlewnictwa*. 59(3), 102-106. (in Polish).